Robust extraction of urinary stones from CT data using attribute filters

Ouzounis, Georgios K.; Giannakopoulos, Stilianos; Simopoulos, Constantinos E.; Wilkinson, Michael H.F.

ROBUST EXTRACTION OF URINARY STONES FROM CT DATA USING ATTRIBUTE FILTERS

Georgios K. Ouzounis,
Stilianos Giannakopoulos,
Constantinos E. Simopoulos *

Michael, H.F. Wilkinson

School of Medicine,
Democritus University of Thrace, University
General Hospital of Alexandroupoli,
68100 Alexandroupoli, Greece

Institute of Mathematics and Computing
Science, University of Groningen,
P.O. Box 407, 9700 AK Groningen,
The Netherlands

ABSTRACT

In medical imaging, anatomical and other structures such as urinary stones, are often extracted with the aid of active contour/surface models. Active surface-based methods have robustness limitations and are computationally expensive. In this paper we present a morphological method based on attribute filters and the newly presented sphericity attribute. The operators involved, extract the targeted objects in their entirety without shape/size distortions and proceed rapidly. Experiments on three real 3D data-sets demonstrate their efficiency and their performance is discussed.

Index Terms— Urinary stones, attribute filters, sphericity.

1. INTRODUCTION

Urinary stones are hard mineral masses usually formed inside the kidneys, in the process of filtering blood to remove liquid waste. Aided by urine, the stones can travel along the urinary tract which apart from the kidneys consists of the ureter, the bladder and the urethra. If small in size, they often are expelled from the body without any noticeable symptoms. In certain cases though, either due to size or shape, they may get stuck inside the kidneys or in other parts of the urinary tract causing severe pain. This condition is known as *urolithiasis* and is diagnosed with the aid of ultrasound (US), helical computerized tomography (CT) or intravenous pyelograms (IVP). All three methods provide visual data assisting the diagnosis, the localization of the stones and possibly pre-operative planning.

Stacks of progressive CT scans can be used to construct 3D models which offer a number of advantages in the visualization of the targeted structures [1]. Extracting urinary stones

from 3D data-sets, like many other segmentation problems in medical imaging, commonly relies on active surfaces [2] or active contours stacked after processing. Active surfaces have three distinctive drawbacks; the require careful, and some times manual initialization, they might converge inaccurately if mislead by noise or other nearby objects and they are computationally expensive due to their iterative nature. Instead, in this paper we propose an alternative, morphological method based on attribute filters. It relies on two filtering steps, one based on the newly presented sphericity attribute and the second on size. We validate it on three different cases dealing with a stone in a kidney, three smaller stones in the ureter and a major stone inside the bladder. The results show that the method extracts all stones present robustly and in their entirety, while the timings suggest a clear speed advantage over other methods. Note that this is not a comparison paper between this method and others; it simply aims to demonstrate the performance of connected morphology in medical imaging. A full comparative study is in progress.

2. ATTRIBUTE FILTERS

2.1. Connectivity Openings and Filters

Attribute filters [3] are a class of edge preserving operators acting on connected image regions instead of individual pixels. They are based on *connectivity openings* [4,5] Γ_x and can either remove or preserve objects in their entirety but cannot introduce new edges. An object in a binary image X, is a set $C_x \subseteq X$ of path-wise connected points, of maximal extent. This means that there cannot be any other set $C'_x \supset C_x$ such that $C'_x \subseteq X$ using the same connectivity rules. C_x in this case is also referred to as a *connected component*. A connectivity opening $\Gamma_x(X)$ given a point $x \in X$, returns the connected component containing x or $\emptyset$ otherwise. It is characterized by the following three properties; for any two sets X, Y it is *anti-extensive* i.e. $\Gamma_x(X) \subseteq X$, it is *increas-*

ing i.e. if $X \subseteq Y \Rightarrow \Gamma_x(X) \subseteq \Gamma_x(Y)$, and *idempotent* i.e. $\Gamma_x(\Gamma_x(X)) = \Gamma_x(X)$. Furthermore, for all $X \subseteq E$, with E being some arbitrary superset, $x, y \in E$, $\Gamma_x(X)$ and $\Gamma_y(X)$ are either equal or disjoint.

Attribute filters work by imposing attribute-based constraints on Γ_x in the form of binary criteria Λ. These are put in place by means of a trivial opening Γ_Λ. The latter yields C_x if $\Lambda(C_x)$ is true, and $\emptyset$ otherwise. Furthermore, $\Gamma_\Lambda(\emptyset) = \emptyset$. They are typically expressed as:

$$\Lambda(C_x) = Attr(C_x) \geq \lambda, \tag{1}$$

with $Attr(C_x)$ being some real-value attribute of C_x, and λ an attribute threshold.

Definition 1 *The binary attribute filter Γ^Λ of a set X with an increasing criterion Λ is given by:*

$$\Gamma^\Lambda = \bigcup_{x \in X} \Gamma_\Lambda(\Gamma_x(X)). \tag{2}$$

An example of increasing attributes and thus increasing criteria is the volume measure. Non-increasing criteria usually rely on shape descriptors such as moment-invariants, elongation, flatness, sparseness, e.t.c. [6]. Connected operators employing such attribute criteria are referred to *shape filters*. To compensate for their non-increasingness they are required to be rotation, translation and scale-invariant [7]. Following we discuss a new shape attribute employed in our method.

2.2. The Sphericity Attribute

Sphericity SPH [8] is a unit-free measure of how spherical an object is. It is quantified by using a unique mathematical property of the sphere; the sphere has the lowest surface-to-volume ratio of any solid geometric objects. Sphericity is defined as the surface area S_e of a sphere of the same volume as the connected component C_x, divided by the actual surface area S_a of C_x, i.e.:

$$SPH = S_e/S_a, \tag{3}$$

Wadell [8] expanded this further by giving the surface area of a sphere S_e, in terms of its volume V.

$$
\begin{aligned}
S_e^3 &= (4\pi r^2) = 4^3\pi^3 r^3 = 4\pi(4^2\pi^2 r^6) \\
&= 4\pi 3^2 \left(\frac{4^2\pi^2}{3^2}r^6\right) = 36\pi(\frac{4\pi}{3}r^3)^2 = 36\pi V^2,
\end{aligned}
\tag{4}
$$

therefore,

$$S_e = (36\pi V2)^{\frac{1}{3}} = \pi^{\frac{1}{3}}(6V)^{\frac{2}{3}}. \tag{5}$$

Substituting into (3) yields:

$$SPH = \frac{\pi^{\frac{1}{3}}(6V)^{\frac{2}{3}}}{S_a} \tag{6}$$

The sphericity measure has a maximum of 1 for a solid sphere and decreases as the object gets more sparse or hollowed.

The actual surface area of a 3D object can be measured in a number of different ways. A problem with most pixel-based methods though, is that they are not rotation invariant. To counter this, estimates of surface area are computed which though they can ensure rotation invariance, cause a rounding effect in corners thus missing the contribution of certain pixels. In our method we used an extension of the city-block perimeter metric to 3D. For every pixel p visited, we retrieve its neighbors and initialize a variable $peri$ to the difference between the maximum number of neighbors (6-way adjacency) and the actual ones. For each neighbor with intensity higher than that of p, $peri$ is incremented and the opposite. After all neighbors are processed, the attribute measure of the connected component visited is updated. Though not rotation invariant, the specific metric was seen to perform satisfactory and was further employed to compute sphericity.

3. EXPERIMENTAL METHOD AND TESTS

Both the volume and surface area attributes are computed using the Max-Tree algorithm [9]. Max-Trees are versatile data structures introduced in the context of anti-extensive attribute filtering. They extend binary operators to gray-scale through the concept of threshold superposition and allow for their efficient computation. A Max-Tree demo [6] for both attribute filtering and 3D visualization is available at our web-site at `http://www.cs.rug.nl/~michael/MTdemo`.

Our method for extracting the urinary stones consists of two filtering steps. The first subjects our test data-sets to the sphericity criterion, preserving only compact structures. A volume opening follows to remove noise and other smaller, compact artifacts. We experiment on three real data-sets, the first and third of which are down-sampled to 8-bit sets, courtesy of the Department of Radiology and Medical Imaging, University General Hospital of Alexandroupolis, Greece.

The first data-set (top row in Fig. 1) is a $512 \times 512 \times 77$, 8-bit volume of the upper abdominal region with a *renal calculus* present at the left kidney. The first image from the left shows an axial ortho-slice in which the stone is visible as a bright disk within the renal pelvis. Setting $\lambda_{SPH} = 0.4$ and $\lambda_V = 460$, the final result of the two filters is shown in the middle image which is an iso-surface projection at iso-level 1. The spikes visible are of low intensity which can either be thin crystal protrusions lodging the stone to the kidney or connected noise particles. To remove them, an open-close operation with a spherical structuring element of a rather small radius is sufficient. The segmented stone superimposed with the spinal cord is shown at the right most image.

The second data-set was acquired in the process of evaluating a pelvic bone disorder. It is a $512 \times 512 \times 125$, 16-bit volume in which, incidentally, a cluster of three urinary stones are visible along the ureter. The first image of the second row
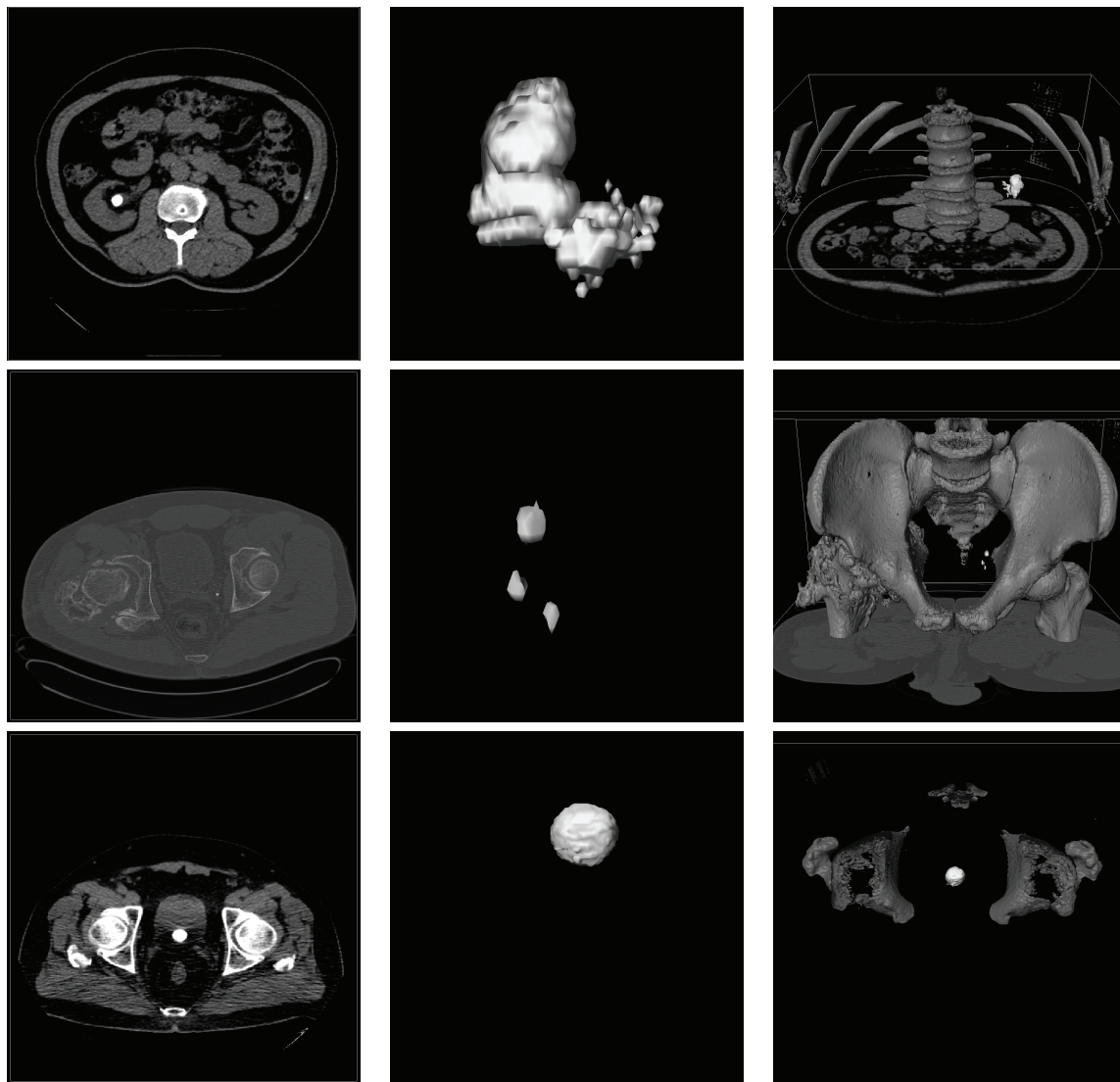
Fig. 1. Axial ortho-slices (CT) of three cases of urinary stones: in a kidney, along the ureter and in the prostate (first column from the left); the extracted stones (second column); the stones superimposed with other anatomical structures (third column).

- Fig. (1) shows the cross-section of one of them, next to the pelvic bone (small bright disk). All three stones are more spherical than the previous case allowing for a higher value for λ_{SPH}. This, removes further noise at the first step already. The filter settings for this set are $\lambda_{SPH} = 0.6$ and $\lambda_V = 5$ and the result is shown at iso-level 5, middle image. The final result is superimposed with an enhanced view of the pelvic bones for localization - right most image.

The third case is of a patient suffering from a urinary bladder stone. The data-set shown in third row of Fig. (1), is a $512 \times 512 \times 31$, 8-bit volume. Using $\lambda_{SPH} = 0.6$ and $\lambda_V = 40$, clears entirely the image leaving the stone alone. It is shown at iso-level 1 in the middle image. The third image, like the two previous cases, shows the segmented result superimposed with parts of pelvic bones for localization.

4. DISCUSSION

Stacks of CT scans used to construct 3D models often contain anisotropic data which have an undesirable effect on the quality of the visualization methods chosen. The data-sets used in the previous section, though not highly anisotropic, have an impact on the filter parameters too, which is particularly noticeable in the last experiment. The stone, even though it appears to be spherical enough to expect a higher λ_{SPH}, it is removed for any value higher than 0.6. If spacing information are not taken into consideration, it can be seen that the stone actually looks more like an oblate spheroid. This is a rotation-

ally symmetric ellipsoid having a polar axis shorter than the diameter of the equatorial circle whose plane bisects it. The sphericity measure of such a spheroid is given by

$$SPH = \frac{2\sqrt[3]{ab2}}{a + \frac{b2}{\sqrt{a2-b2}}ln(\frac{a+\sqrt{a2-b2}}{b})},\qquad(7)$$

where a, b are the *semi-major* and *semi-minor* axes respectively. As b gets smaller the volume is reduced at a higher rate than the surface area, thus SPH reduces too. Additionally, it can be shown that in the case of isotropic voxels, the area of a sphere is approximated in the 6-neighbor case as $\frac{6}{\pi}r^2$ (the surface seen face-on times the six faces). This means that the sphericity of a digital sphere is $4/6$ in this case while for an axis aligned cube it is 0.82, as expected. Both factors are countered in an anisotropy-invariant volume and surface area metric (also rotation invariant), currently under development.

For the second data-set, using any higher λ_{SPH} removes the lower two stones which are not as spherical as the top one. In the first data-set the stone is not very spherical but sufficiently compact to be differentiated from the rest of the anatomical structures. The small, thin protrusions if judged necessary for volumetric purposes but undesired in visualization, they can be removed from the scene by increasing the iso-level. Since they do not contain as much calcium as the main body of the stone, they do not reflect much radiation and thus are of low intensity.

The timings of all three experiments where taken on a system with an Intel(R) Core2 CPU T7400 @ 2.16 GHz processor and 2GB RAM, running Windows XP. For each volume the first set gives the time (sec.) taken for building and filtering the Max-Tree with the sphericity attribute and the second for the volume attribute. Kidney stone: (27.359,0.563), (18.859,0.484); ureter stones: (46.844,1.797), (32.219,1.468); bladder stone: (9.375,0.203), (6.359,0.188). Computing the sphericity attribute takes approximately 1.5 times longer than the volume attribute which is explained by the algorithm's demand to revisit each voxel's 6-neighborhood for computing the surface measure.

5. CONCLUSIONS

In this paper we used two connected attribute filters based on the sphericity and volume attributes to isolate urinary stones from CT data-sets. Our method, apart from its simplicity has three major advantages; the edges of the extracted stones remain intact after filtering, there is no pre-processing or initialization required and the filters are computed in very short times given the size of the data-sets. The filters operate directly on 3D data and the filter parameters can be changed interactively without re-computing the Max-Tree structure [6].

In future work, we aim at improving the surface metric. A further study of more complicated cases of kidney stones is also being carried out. Kidneys may have several stones and

of varying size and shape while other artifacts may co-exist, satisfying both criteria. To handle such cases we are looking at generalized notions of connectivity such as in [10]. Moreover, a comparative study between this and active surface-based methods should be carried out to quantify the advantages in both speed efficiency and robustness.

6. REFERENCES

[1] N. P. N. Buchholz, "Three-dimensional ct scan stone reconstruction for the planning of percutaneous surgery in a morbidly obese patient.," *Journal of Endourology.*, vol. 16, no. 4, pp. 215–220, 2000.

[2] A. Osorio, O. Traxer, S. Merran, F. Dargent, X. Ripoche, and J. Atif, "Real time fusion of 2d fluoroscopic and 3d segmented ct images integrated into an augmented reality system for percutaneous nephrolithotomies (pcnl)," in *RSNA'04*, Chicago, USA, November 28-December 3 2004.

[3] E. J. Breen and R. Jones, "Attribute openings, thinnings and granulometries," *Comp. Vis. Image Understand.*, vol. 64, no. 3, pp. 377–389, 1996.

[4] J. Serra, Ed., *Image Analysis and Mathematical Morphology. II: Theoretical Advances*, Academic Press, London, 1988.

[5] C. Ronse, "Set-theoretical algebraic approaches to connectivity in continuous or digital spaces," *Journal of Mathematical Imaging and Vision*, vol. 8, pp. 41–58, 1998.

[6] M. A. Westenberg, J. B. T. M. Roerdink, and M. H. F. Wilkinson, "Volumetric attribute filtering and interactive visualization using the max-tree representation," *IEEE Trans. Image Proc.*, vol. 16, no. 12, pp. 2943–2952, 2007.

[7] E. R. Urbach, J. B. T. M. Roerdink, and M. H. F. Wilkinson, "Connected shape-size pattern spectra for rotation and scale-invariant classification of gray-scale images," *IEEE Trans. Pattern Anal. Mach. Intell.*, vol. 29, no. 2, pp. 272–285, 2007.

[8] H. Wadell, "Volume, shape and roundness of quartz particles," *Journal of Geology*, vol. 43, pp. 250–280, 1935.

[9] P. Salembier, A. Oliveras, and L. Garrido, "Anti-extensive connected operators for image and sequence processing," *IEEE Trans. Image Proc.*, vol. 7, pp. 555–570, 1998.

[10] G. K. Ouzounis and M. H. F. Wilkinson, "Mask-based second-generation connectivity and attribute filters," *IEEE Trans. Pattern Anal. Mach. Intell.*, vol. 29, no. 6, pp. 990–1004, 2007.